JCIS Open 9 (2023) 100078

Contents lists available at ScienceDirect

JCIS Open

journal homepage: www.journals.elsevier.com/jcis-open

Low doses of pharmaceutical formulations loaded with UFMG-V4N2 immunogen induce the production of IgG anti-cocaine antibodies and provide evidence of cerebral protection in the preclinical model

Bruna Rodrigues Dias Assis [a], Paulo Sérgio de Almeida Augusto [b,c], Raissa Lima Gonçalves Pereira [b,c], Sordaini Maria Caligiorni [b], Brian Sabato [b,d], Larissa Pires do Espírito Santo [b,d], Karine Dias dos Reis [b], Leonardo da Silva Neto [e,g], Simone Odília Antunes Fernandes [f], Valbert Nascimento Cardoso [f], Maila Castro Lourenço das Neves [b,d], Ângelo de Fátima [g], Frederico Duarte Garcia [b,c], Gisele Assis Castro Goulart [a,*]

[a] Department of Pharmaceutics, UFMG, Brazil
[b] Department of Mental Health, UFMG, Brazil
[c] Pós-graduação em Medicina Molecular, UFMG, Brazil
[d] Pós-graduação em Neurociências, UFM, Brazil
[e] Instituto Federal Farroupilha, Alegrete, Brazil
[f] Department of Clinical & Toxicological Analysis, UFMG, Brazil
[g] Department of Chemistry, UFMG, Brazil

ARTICLE INFO

Handling Editor: Prof Qiang He

Keywords:
UFMG-V4N2
calix[4]arene-based immunogen
Pharmaceutical formulation
Anti-cocaine therapy

ABSTRACT

Anti-cocaine vaccines are a promising therapeutic strategy for treating cocaine use disorders. Here we hypothesize that nanoemulsions (NE) or suspensions (SS) loaded with the calix [4]arene-based immunogen UFMG-V4N2 can induce the production of anti-cocaine antibodies and decrease the passage of radiolabeled cocaine analog [^{99m}Tc] Trodat-1 through of the brain barrier. UFMG-V4N2 was characterized (solubility, morphology, DSC, XRD) and loaded into NEs and SSs using excipients approved for human use. Immunogenic efficacy was assessed by quantifying the titers and determining the specificity of anti-cocaine IgG antibodies, and by assessing the inhibition of [^{99m}Tc]Trodat-1 trafficking across the mice brain-barrier. UFMG-V4N2 is an amorphous, thermally stable molecule with very low hydrophilicity. The immunogenicity of NE or SS was similar, but aluminum phosphate and the lower dose of UFMG-V4N2 induced higher anti-cocaine IgG antibody titers, minimizing [^{99m}Tc]Trodat-1 uptake in the brain. Therefore, the UFMG-V4N2 may represent an alternative for the treatment of cocaine use disorder.

1. Introduction

Anti-cocaine vaccines are a promising therapeutic strategy for the treatment of cocaine use disorders, which are associated with cognitive and behavioral changes, making individuals more impulsive and prone to aggressive acts and criminality, in addition to a higher incidence of deaths and suicides [1,2]. Previous studies of anti-cocaine vaccines used protein-based immunogens, such as hemocyanin (KLH) [3,4], bovine serum albumin (BSA) [5] and adenovirus capsid (Ad) [6].

Although conventional protein-based immunogens are extensively used in vaccine development and have been highly efficacious for several decades in reducing mortality and morbidity due to infectious disease, the immunogenicity of the protein-based therapeutics can trigger an unwanted immune response and require a more complex production process and cold-chain of supply [7,8]. Aiming to solve these issues, a new calix [4]arene-based anti-cocaine immunogen called UFMG-V4N2 was synthesized. The UFMG-V4N2 yielded titers of anti-cocaine antibodies following the mice vaccination sufficient to decrease the passage

* Corresponding author. Faculty of Pharmacy, Department of Pharmaceutics, UFMG, Campus Pampulha, Av Antônio Carlos, 6627, CEP 31270, Belo Horizonte, MG, Brazil.
E-mail addresses: giseleacgoulart@gmail.com, gacg@ufmg.br (G.A.C. Goulart).

https://doi.org/10.1016/j.jciso.2023.100078
Received 24 June 2022; Received in revised form 23 November 2022; Accepted 19 January 2023

of a radiolabeled cocaine analog ([^{99m}Tc]Trodat-1) into the animal brain [9]. However, in previous preclinical studies that evaluated UFMG-V4N2, the formulation was composed of saline, dimethylsulfoxide and Freund's adjuvant [9]. This formulation does not comply with the requirements for human use. For this study, we focused on developing a formulation with components approved by international regulatory agencies for human use, which may facilitate the passage from the preclinical to clinical phases of vaccine development. These components were used to produce two pharmaceutical formulations: a suspension (SS) and a nanoemulsion (NE).

Most vaccines are marketed as a solution and SS, but since the 2000s, several NE-based adjuvants have been developed, and some are already marketed [7,10]. NEs are inexpensive, easily produced emulsions with internal droplet sizes in the nanometer range (20–600 nm), usually 20–200 nm [11]. Immunological adjuvants are also an important component of vaccine formulations, as they can enhance the effectiveness of the immune response, with aluminum hydroxide (AH) and aluminum phosphate (AP) being the most used due to their good safety record [12,13].

We hypothesize that these novel formulations, developed with approved excipients and adjuvants, may induce the production of anti-cocaine IgG antibodies and decrease the passage of a radiolabeled cocaine analog ([^{99m}Tc]Trodat-1) through the mice brain barrier. To assess this hypothesis, we first performed the physicochemical characterization of three batches of UFMG-V4N2, then we developed two different pharmaceutical formulations (NE and SS) and compared immunogenicity in a pre-clinical model using two types of aluminum salts (AH and AP) and two different doses of UFMG-V4N2.

2. Materials and methods

2.1. Chemicals and reagents

The UFMG-V4N2 immunogen and the hydrolysis-tolerant hapten GNE [(6-(1*R*,2*R*,3*S*, 5*S*)-3-(benzoyloxy)-8-methyl-8-azabicycle [3.2.1] octane-2-carboxamide-hexanoic acid)] were synthesized and supplied by our research group and stored at 2–8 °C [9]. Polysorbate 80, sesame oil, propylene glycol, polyethylene glycol 300, poloxamer, and span 80, all super refined grades, were supplied by Croda Inc® (Mill Hall, Pennsylvania, USA). Merck KgaA (Darmstadt, Germany) provided absolute ethanol and benzyl alcohol Emprove® Expert. Croda® (Frederikssund, Denmark) supplied the Adju-phos® (AP, 5 mg/mL) and the Alhydrogel® 2% (AH, 10 mg/mL) adjuvants. The study used an adjuvant's final aluminum concentration of 0.5 mg/mL, below the regulatory limit of 0.85–1.25 mg/mL [14]. The complete and incomplete Freund's adjuvant was purchased from Merck-Sigma (St. Louis, USA). All chemicals were of analytical grade.

2.2. Characterization of UFMG-V4N2 immunogen

The solubility of UFMG-V4N2 was evaluated by titration in acetonitrile, water, absolute ethanol, benzyl alcohol, dimethyl sulfoxide, methanol and different associations of solvents and cosolvents. Solubility classification in each solvent was performed as recommended by the US Pharmacopeia's (USP) [15].

Thermogravimetric and differential scanning calorimetry (DSC) analyses of three different batches of UFMG-V4N2 (B1, B2 and B3) were carried out in the Q5000 thermogravimetric analyzer and in the DSC Q2000 (TA Instruments®, New Castle, USA), respectively. The thermogravimetric studies used a nitrogen gas atmosphere and a heating range from 0 to 800 °C. The DSC analysis used helium gas atmosphere and a temperature range from 0 to 250 °C. Both analyses used a heating ramp of 10 °C/min and a flow rate of 50 mL/min. X-Ray Diffraction (XRD) analyses of UFMG-V4N2 (batches B1, B2 and B3) were performed using an XRD-6000 powder X-ray diffractometer (Shimadzu®, Japan) equipped with a scintillation detector. The samples were analyzed using a current of 30 mA and a voltage of 40 kV. Continuous scan mode (10° to 80° 2Θ, 0.02° sampling step) was used at a scan speed of 1,000°/min. The aperture of the divergence and scattering slits was 1°, while the width of the reception slit was 0.3 mm.

The morphology of UFMG-V4N2 was evaluated by polarized light microscopy (PLM) and scanning electron microscopy (SEM). For PLM, the UFMG-V4N2 was dispersed in water and analyzed using a polarized light microscope (Zeiss Axio Imager. M2, Carl Zeiss, Oberkochen, Germany) equipped with an AxioCam digital camera (Model ERc 5 S, Carl Zeiss, Oberkochen, Germany). For SEM analyses, the UFMG-V4N2 was bonded to a stub, subjected to gold/palladium metallization, and analyzed using a Quanta 3D FEG high-resolution microscope (FEI Company®, Oregon, USA) at an accelerating voltage of 15 Kv. SEM analyses were performed at the Microscopy Center at Universidade Federal de Minas Gerais, Brazil (http://www.microscopia.ufmg.br).

2.3. Formulation's development and characterization

The NEs were prepared by the hot-ultrasound emulsification method, being composed of an oil phase [5 mg/mL benzyl alcohol, 5 mg/mL absolute ethanol, 10 mg/mL sesame oil and 5 mg/mL Span 80] and an aqueous phase (10 mg/mL polysorbate 80, sodium chloride to adjust the osmolality to 280–300 mOsm and water for injection). Briefly, the aqueous phase (AP) and the oil phase (OP) were heated separately to 70 °C and the AP was slowly poured into the OP, under agitation (8000 rpm, 2 min), using an Ultra Turrax T-25 homogenizer (Ika Labortechnik®, Germany). Next, the emulsion was submitted to 10 min of tip sonication (21% amplitude, Ultra-cell 750 W, Sonics Materials Inc, USA). The NEs were cooled in a water bath until reaching room temperature and pH was adjusted to close to 7.0 (6.5–7.5). Five types of NEs were produced: 1. NE without UFMG-V4N2 (NE blank); 2. NE loaded with 0.1 mg/mL of UFMG-V4N2 (NE-UFMG-V4N2); 4. NE loaded with 0.1 mg/mL of UFMG-V4N2 and AH (NE-UFMG-V4N2-AH); and 5. NE loaded with 0.1 mg/mL of UFMG-V4N2 and AP (NE-UFMG-V4N2-AP).

The SSs were prepared by the complete solubilization of UFMG-V4N2 in ethanol absolute (10 mg/mL), followed by the addition of propylene glycol (120 mg/mL), polyethylene glycol 300 (180 mg/mL), polysorbate 80 (0.05 mg/mL), water for injection and the suspension of aluminum salts (AH or AP). It is important to highlight that, before adding the aluminum salts, we had a solution (S) where all the excipients and the UFMG-V4N2 were fully solubilized. At the end of production, the pH of all SS was adjusted to close to 7.0 (6.5–7.5). Two solutions (S) and three suspensions (SS) were produced: 1. S without UFMG-V4N2 (S-blank); 2. S with 0.1 mg/mL of UFMG-V4N2 (S-UFMG-V4N2); 3. SS with 0.1 mg/mL of UFMG-V4N2 and AH (SS-UFMG-V4N2-AH); 4. SS with 0.1 mg/mL of UFMG-V4N2 and AP (SS-UFMG-V4N2-AP); 5. SS with 6.74×10^{-5} mg/mL of UFMG-V4N2 (SS-UFMG-V4N2 LD-AP). In the second *in vivo* study, the SS with 0.1 mg/mL of UFMG-V4N2 was named SS-UFMG-V4N2 HDAP.

For the *in vivo* studies, we also prepared formulations with GNE-KLH (First study) or UFMG-V4N2 (Second study) in CFA (first dose) or IFA (booster doses). These formulations were used as a positive control and were prepared as described in Neto and Maia et al. [9].

Particles/globules size and polydispersity index (PDI) of formulations were determined by dynamic light scattering (DLS) using a Zetasizer Nanoseries Nano-ZS90 (Malvern Instruments, UK), at a fixed angle of 90° and at 25 °C. The Zeta potential was evaluated by electrophoretic light scattering technique, using the same equipment. The osmolarity of all formulations was evaluated in a cryoscopic osmometer (Osmomat 030, Gonotec, Germany). The SSs were previously diluted in water (1:10) and the NEs were analyzed without previous dilution.

2.4. Animals and experimental groups

The experiments were carried out in accordance with the UFMG Ethics Committee on Animal Experimentation (CEUA/UFMG nº 122/

2016), with the ARRIVE guidelines and EU Directive 2010/63/EU. For both studies, male Balb-C mice (4–5 weeks, 20–25 g, Central vivarium - UFMG, Brazil) were housed in Makrolon cages and kept in a ventilated room (22 ± 1 °C, light/dark cycle of 12 h) with ad libitum feed and water. Animals were randomly assigned to each group using the Excel's basic random number generator. The researchers who performed the animal experiments and statistical analysis were unaware of the injected treatment. Researchers not involved in the animal experiments prepared the vaccine and placebo formulations. The treatments were delivered in numbered vials and with the necessary volumes for each application. The identification of treatments was disclosed at the end of the statistical analysis to the main investigator.

In the first experiment, 30 male BALB/c mice were randomly allocated into eight groups (n = 3 animals): 1. GNE-KLH (Positive control); 2. NE-blank (Negative control); 3. S-UFMG-V4N2; 4. NE-UFMG-V4N2; 5. SS-UFMG-V4N2-AP; 6. SS-UFMG-V4N2-AH; 7. NE-UFMG-V4N2-AP; 8. NE-UFMG-V4N2-AH. The immunogen formulations contained 0.1 mg/mL of UFMG-V4N2 and 0.5 mg/mL of aluminum (AH or AP). The GNE-KLH homogenized in CFA (first vaccine dose) or IFA (booster doses), was standardized in previous studies as a positive control [4,9] and used in the first study to maintain the reference. The second study used UFMG-V4N2-FA (CFA-first dose or IFA-booster doses) instead of GNE. This modification occurred to assess whether UFMG-V4N2 in CFA or IFA would be able to induce similar titers of anti-cocaine antibodies to those observed for GNE-KLH (first study). In the second study, 42 male BALB/c mice were randomly allocated into four groups (n = 10–12 animals): 1. UFMG-V4N2-FA (CFA-first dose or IFA-booster doses) (positive control); 2. S-blank (negative control); 3. SS-UFMG-V4N2 LD-AP (6.74×10^{-5} mg UFMG-V4N2/mL); 4. SS-UFMG-V4N2 HD-AP (0.1 mg UFMG-V4N2/mL). The abbreviations LD and HD stand for low and high doses, respectively. For both studies (1 and 2) each animal received 0.3 mL of formulation, intraperitoneal (i.p.) injection, on days 0, 7, 21, 28, and 42. Blood samples were collected via the submandibular vein (days 0, 7, 14, 21, 28, 42, and 50 - first study; days 0, 7, 21, 28, 35, 42, and 50 - second study). The collected blood was centrifuged (20 min, 2400 rpm, 4 °C) and the serum was aliquoted and frozen (−80 °C) until analysis.

2.5. Indirect enzyme-linked immunosorbent assay (ELISA)

For the ELISA assay, Maxisorp plates (Nunc, Rochester, NY), were fixed for 24 h at 4 °C with 100 µL/well of a cocaine solution (2 mg/mL) diluted in a buffer consisting of 0.05 M Na_2CO_3, 0.05 M $NaHCO_3$ and 0.02% sodium azide (pH 9.6). After washing the plates, 100 µL of serum samples diluted in buffer (1:200, PBS and 0.02% sodium azide) were transferred to the respective wells and kept in incubation at 4 °C overnight. The plates were washed again and incubated with 100 µL of anti-mouse IgG alkaline phosphatase conjugate (1:2000) (Sigma, St. Louis, MO, USA) for 3 h at 37 °C. After washing, 100 µL of 4-nitrophenyl phosphate disodium salt hexahydrate solution (Sigma, St. Louis, MO, USA) was transferred to each well, and the plates were kept in the shade of light for 40 min until the reaction was interrupted with 50 µL/well of NaOH (3 N). The plate was read at 405 nm in a multi-mode Varioskan LUX microplate reader (Thermo Fisher Scientific, MA).

2.6. Adsorption ELISA

To assess the specificity for anti-cocaine IgG, an adsorption assay was performed by incubating the serum samples with free cocaine. Before addition to the plate, serial dilutions (10^{-10}, 10^{-8}, 10^{-6}, 10^{-4}, 10^{-3}, 10^{-2} mg/mL) were incubated for 2 h with serum samples diluted 1/200 in sample buffer. The results obtained are presented as a plot of optical density (OD) vs logarithmic cocaine concentration.

2.7. Anti-cocaine IgG titer determination

Anti-cocaine IgG antibody titers were calculated using the indirect ELISA protocol with cocaine 2 mg/mL adsorbed on the solid phase. Serum samples were serially diluted (1/50 to 1/51.200). The titer corresponded to the inverse of the serum dilution required to generate a half-maximal response upon antigen binding.

2.8. Brain tissue scintigraphy

On 43rd day after the last booster, 27 mice from the second study (i.e., S-blank, SS-UFMG-V4N2 AP-HD and SS-UFMG-V4N2-AP-LD, n = 9) received 0.1 mL of [^{99m}Tc] Trodat-1® solution (4.81 MBq/130 µCi) in the tail vein. After 90 min, the animals received an anesthetic mixture of ketamine (80 mg/kg) and xylazine (15 mg/kg) and were placed in the gamma-camera (Nucline™, Mediso, Hungary) in dorsal decubitus position. The scintigraphic images of the total radiation count in the mice brain were obtained and worked out by the equipment's software (Mediso InterView XP, Hungary).

2.9. Statistical design and analysis of data

Results were represented as mean ± standard deviation of the mean. The normal distribution of data was assessed by the Shapiro-Wilk test. Means were compared between groups using the *one-way* ANOVA test, followed by Tukey's post-test; except for osmolality data, which were evaluated using the Kruskal-Wallis test followed by the Dunn test. To verify the interaction between the independent variable time and treatment in the *in vivo* study, *two-way* ANOVA followed by Tukey's post-test was used. Values of $p < 0.05$ were considered significant. The IC50 values were obtained by non-linear regression. Statistical analyses were performed using GraphPad Prism Software®, version 8.2.1 (San Diego, USA). To calculate the sample size, the G-Power 3.1® software was used. The primary outcome of both experiments was the anti-cocaine IgG titer on day 21, which corresponds to the peak of antibody production [4,9]. In the first study, the impact of two types of formulations and adjuvants on the induction of IgG anti-cocaine antibodies was evaluated in comparison with the positive control group (GNE-KLH). Therefore, we based on the study carried out by de Almeida et al. [4], which used GNE-KLH. The sample size was calculated considering the mean and standard deviation of the vaccinated and placebo groups 21 days after the first injection of GNE-KLH, which was the point where there was the greatest difference between the groups and the highest level of IgG anti-cocaine antibodies (vaccinated group: 3.413 ± 0.073; placebo group: 0.422 ± 0.388). Considering the effect size, α error = 0.05 and power = 0.95, the sample size calculated for each group was = 2. Thus, in the first study, we used a sample size = 3–4 mice. For the second study, in which only UFMG-V4N2 was used as immunogen, we based the sample size calculation on the study carried out by Neto and Maia et al. [9], where the following values were found: 1.3829 ± 0.4506 (vaccinated group) and 0.7690 ± 0.3052 (placebo group). The sample size was calculated as described for the first study and resulted in a sample size = 10–12 mice.

3. Results

3.1. Characterization of UFMG-V4N2

The solubility studies showed that UFMG-V4N2 is practically insoluble in water, presenting a solubility of 10 mg/mL in benzyl alcohol and ethanol absolute. Both solvents are approved for parenteral administration in humans [16] and were selected for the formulations development. Images obtained by polarized light microscopy and scanning electron microscopy were used to evaluate the morphology of UFMG-V4N2 (Fig. 1A–C). In the polarized light images (Fig. 1A and B) it is possible to observe irregular structures without light polarization, suggesting that UFMG-V4N2 is organized in an amorphous structure. SEM images (Fig. 1C) showed particles with a wide range of sizes and a plaque-like morphology, with irregular shapes, ranging from approximately 2 to 523 µm.

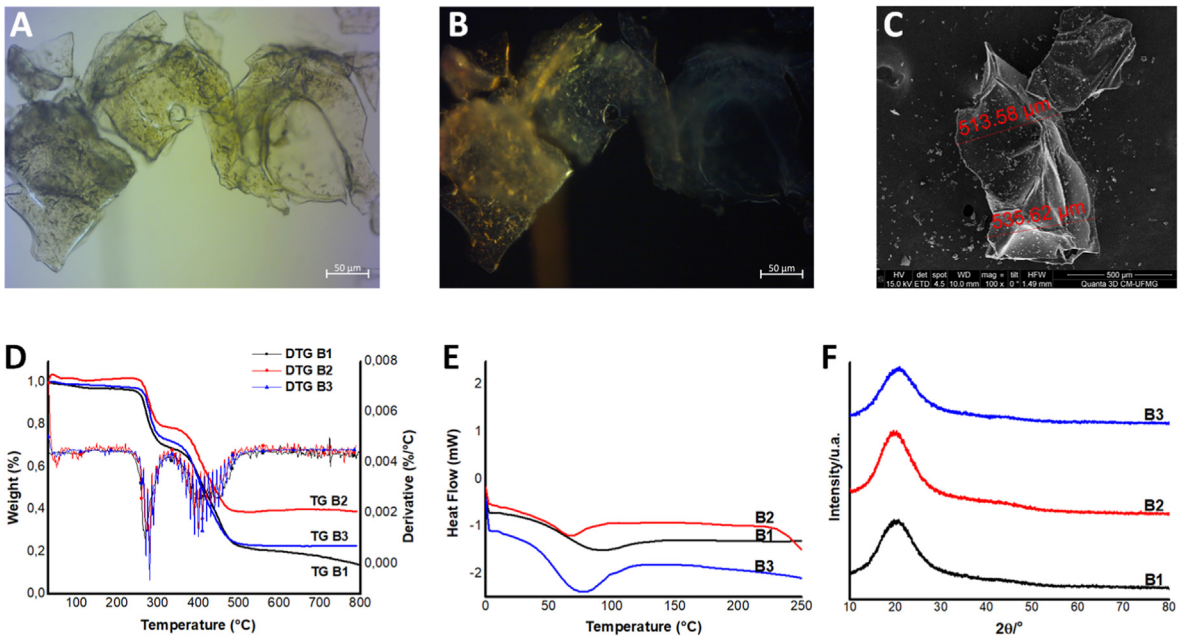

Fig. 1. Characteristics of the UFMG-V4N2. **A,B.** Polarized light microscopy images in bright (**A**) and dark (**B**) fields. **C.** Scanning electron microscopy image (× 100). **D.** Thermogravimetric (TG, solid line) and thermogravimetric derivative (DTG, cracked line) curves. **E.** Differential exploratory calorimetry curves. **F.** Powder X-ray diffractograms. Analyses were performed on three different batches of the UFMG-V4N2 immunogen (B1, B2, and B3).

Thermogravimetric analysis (TG, DTG, and DSC) and XRD assessed the thermal behavior and crystallographic structure of three different batches of UFMG-V4N2 (Fig. 1D–F). The TG curves (solid line, Fig. 1D) show a slight mass loss between room temperature and 100 °C ($\overline{X}$ = 0.98%). This finding, also observed in the DTG curves (cracked line, Fig. 1D), probably corresponds to the presence of moisture, water, or residual solvents in the samples. In the range of 100 °C and 246 °C, the sample slowly lost small amounts of mass ($\overline{X}$ = 1.35%), corresponding either to the UFMG-V4N2 degradation or the presence of some solvent. The most significant mass decrease occurs between 246 °C and 321 °C ($\overline{X}$ = 24.31%), when it is possible to observe the thermal degradation of the compound; and between 321 °C and the end of the analysis ($\overline{X}$ = 48.52%), when thermal decomposition of the intermediate formed at 321 °C or of the remainder of the original compound occurs. At the end of heating, an average residue (char) of 25.34% was obtained, corresponding to the residue of carbonized organic matter.

The DTG curves (cracked line, Fig. 1D), parallel to the TG curves (solid line, Fig. 1D), show a small endothermic peak at the beginning of the analysis and two other more prominent endothermic peaks. Both thermogravimetric studies strongly suggest that the decomposition of UFMG-V4N2 begins near 246 °C, and it is not necessary to extend the DSC analysis to temperatures above 246 °C. The DSC analysis (Fig. 1E) showed an extended endothermic event at the beginning of the curve, corresponding to the first step of the TG curves, which may refer to moisture, water, or residual solvent evaporation. This event occurs near 90 °C for batch 1, 65 °C for batch 2, and 75 °C for batch 3. Subsequently, no significant event was observed up to approximately 246 °C. The XRD diffractograms of UFMG-V4N2 presented Bragg reflections at 2Θ positions, with only angular bands identified at 2Θ, characterized by diffuse intensities (Fig. 1F). These diffusely scattered regions are commonly called amorphous halos, being characteristic of X-ray scattering of amorphous material, providing evidence that UFMG-V4N2 is an amorphous substance.

3.2. Development and characterization of formulations loaded with UFMG-V4N2

The formulations were developed using excipients approved for parenteral use, as detailed in the methods section. The NEs presented a milky white appearance (Fig. 2A), while the S and SSs were translucent (Fig. 2B). Before adding aluminum salts, as UFMG-V4N2 and all excipients were utterly solubilized, we had a S. Therefore, some opacity appeared when aluminum salts were added, forming the SSs. The SSs with AH were less opaque than those with AP because the aluminum concentration in the adjuvants is different, 10 mg/mL for AH and 5 mg/mL for AP. Therefore, to reach 0.5 mg/mL of aluminum in the formulations, it was necessary to add twice as much AP, resulting in more suspended material. The pH of the NEs and SSs ranged between 6.5 and 7.3, being close to the physiological pH and the previously established range (6.5–7.5).

The size of NEs globules ranged from 190 to 300 nm (Fig. 2C) and no statistical difference was observed between NEs-blank (191 ± 2 nm) and NE-UFMG-V4N2 (219 ± 0.7 nm, p = 0.6956); nor in relation to NE-UFMG-V4N2-AH (247 ± 17.0 nm, p = 0.1038). However, the mean size of NE-UFMG-V4N2-AP globules (295 ± 4 nm) was statistically different from NE-blank (p = 0.0018) and NE-UFMG-V4N2 (p = 0.0193). There was no statistical difference between NE-UFMG-V4N2-AP and NE-UFMG-V4N2-AH (p = 0.2093).

The SSs showed larger average particle sizes, ranging between 1400 and 2500 nm, about 8 times larger than the NEs globules (p < 0.0001) (Fig. 2C). As observed for NEs, the addition of AP resulted in a larger particle size (2470 ± 54 nm) than the addition of AH (1407 ± 6 nm; p < 0.0001). For SSs, we evaluated the size and ZP only for formulations with aluminum salts (Fig. 2D), because before this addition we had a solution (Fig. 2B).

Regarding the PDI, all developed formulations presented values ranging from 0.30 to 0.15, suggesting a monodisperse system [17]. There was no significant difference between the PDIs (p > 0.05), except for SS-UFMG-V4N2-AP, which presented a lower PDI (0.16 ± 0.07) compared to the other groups (p < 0.05). For ZP (Fig. 2D), a statistical difference was observed between NE-UFMG-V4N2 (−33 ± 0.25 mV) and NE-blank (−42 ± 1 mV; p = 0.0058) and NE-UFMG-V4N2-AP (−23 ± 3 mV; p = 0.0005). The formulations NE-UFMG-V4N2-AH (−5 ± 1 mV) and SS-UFMG-V4N2-AH (25 ± 4 mV), which presented very low or positive ZP, respectively, were statistically different from the other formulations (p < 0.0001). However, there was no statistical difference

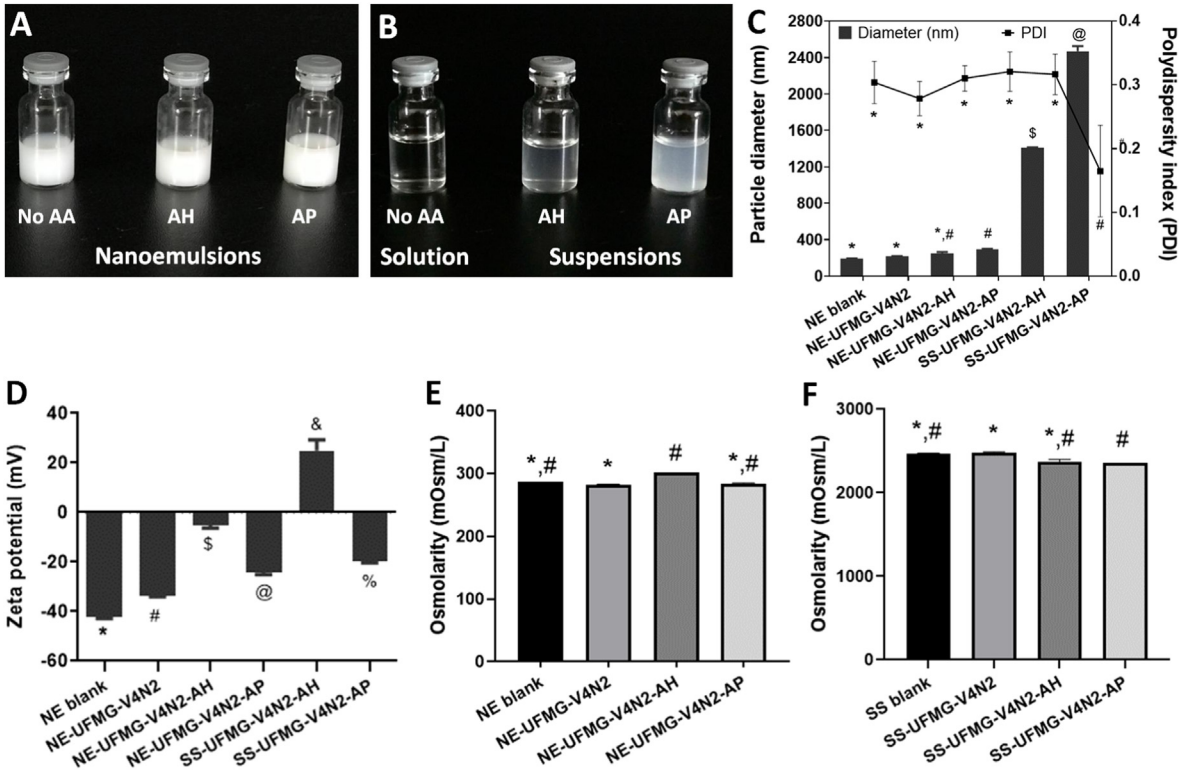

Fig. 2. Characteristics of pharmaceutical formulations loaded with UFMG-V4N2. **A.** Nanoemulsion (NE) without aluminum adjuvant (No AA), with aluminum hydroxide (AH) and with aluminum phosphate (AP). **B.** UFMG-V4N2 solution and suspensions (SS) obtained after the addition of AH or AP. **C.** Particles/globules size and polydispersity index. **D.** Zeta potential. **E,F.** Osmolarity (mOsm/L) of NE (**E**) and of SS (**F**). Data are shown as mean ± standard deviation (n = 3). Different symbols represent $p < 0.05$.

between NE-UFMG-V4N2-AP (−23 ± 3 mV) and SS-UFMG-V4N2-AP (−20 ± 1 mV, $p = 0.5532$).

The osmolality of NEs ranged between 282 and 302 mOsm/kg (Fig. 2E), being close to the plasma osmolality (290 mOsm/kg) [18]. Statistical difference was observed between the NE-UFMG-V4N2 (282 mOsm/kg) and the NE-UFMG-V4N2-AH (302 mOsm/kg, $p = 0.0114$). The SSs presented values ranging from 2360 to 2483 mOsm/kg (Fig. 2F) and the statistical difference was observed only between SS-UFMG-V4N2 (2483 mOsm/kg) and SS-UFMG-V4N2-AP (2360 mOsm/kg, $p = 0.0361$).

3.3. NEs and SSs loaded with UFMG-V4N2 induce anti-cocaine antibodies and minimized the brain entrance of a radiolabeled cocaine analog

We next explore the immunogenic potential of NEs and SSs with two types of aluminum salts in two *in vivo* studies. The anti-cocaine IgG titers do not statistically differ between the groups immunized with the different NEs (Fig. 3B) or SSs (Fig. 3C). However, AP showed a trend towards higher induction of anti-cocaine antibodies production compared to formulations with AH for both formulations (NE and SS). On day 28, the group immunized with NE-UFMG-V4N2-AP presented a higher mean antibody titer than NE-blank ($p = 0.0145$) and NE-UFMG-V4N2 ($p = 0.0274$). Anti-cocaine IgG titer was statistically different from that observed on day 0 ($p = 0.0002$), day 7 ($p = 0.0010$) and day 21 ($p = 0.0047$). On day 50, although there was no statistical difference between the immunized and control groups, the groups immunized with NE-UFMG-V4N2-AP and GNE-KLH had slightly higher IgG anti-cocaine antibody titers than the other groups. In addition, a significant difference between days 0 and 50 was observed for the NE-UFMG-V4N2-AP ($p = 0.0294$) and GNE-KLH ($p = 0.0119$) groups (Fig. 3B).

On day 28, the anti-cocaine IgG titers from the group immunized with SS-UFMG-V4N2-AP were statistically higher than those immunized with S-UFMG-V4N2 ($p = 0.0200$). Furthermore, for the group immunized with SS-UFMG-V4N2-AP, significant differences were also observed between the 28th and 0th ($p = 0.0014$), 7th ($p = 0.0056$) and 21st ($p = 0.0300$); as well as on day 50 compared to day 0 ($p = 0.0401$). Unlike the group immunized with NE-UFMG-V4N2-AH, the group immunized with SS-UFMG-V4N2-AH had high antibody titers on day 28, which was statistically different from day 0 ($p = 0.0258$). The group immunized with GNE-KLH (positive control) presented statistical differences in anti-cocaine IgG titers when comparing day 50 with day 0 ($p = 0.0456$) (Fig. 3C).

In the second *in vivo* study, the immunogenic effects of two doses of SS-UFMG-V4N2 were compared (Fig. 3D). As can be seen, up to day 21, the positive control group (UFMG-V4N2-FA) had higher anti-cocaine IgG titers, although with no significant difference with the other groups. However, from day 35, the group immunized with SS-UFMG-V4N2-LD-AP had higher anti-cocaine IgG titers, which were significantly different from the groups that received S-blank (day 35, $p < 0.0001$; day 50, $p = 0.0028$), UFMG-V4N2-FA (day 35, $p = 0.0634$) and SS-UFMG-V4N2 HD-AP (day 35, $p = 0.0005$; day 50, $p < 0.0001$). On day 50, the group immunized with SS-UFMG-V4N2-HD-AP had the highest antibody titer, being statistically different from the group treated with S blank ($p = 0.0034$) and positive control group (UFMG-V4N2-FA, $p = 0.0018$), but not significantly different from the group immunized with SS-UFMG-V4N2-FA ($p = 0.5734$).

The midpoint anti-cocaine IgG antibodies titer was determined for animals immunized with the SS-UFMG-V4N2-LD-AP (Fig. 3E) and a titer about 1:400 was obtained. In Fig. 3F, the adsorption assay shows that the antibodies found in the serum of mice immunized with SS-UFMG-V4N2-LD-AP are specific for cocaine, with a greater binding of these antibodies to cocaine being observed.

To assess whether the titer of anti-cocaine IgG antibodies observed in the immunized groups could reflect less cocaine in the animals' brain, we evaluated the passage of a radiolabeled cocaine analog through the

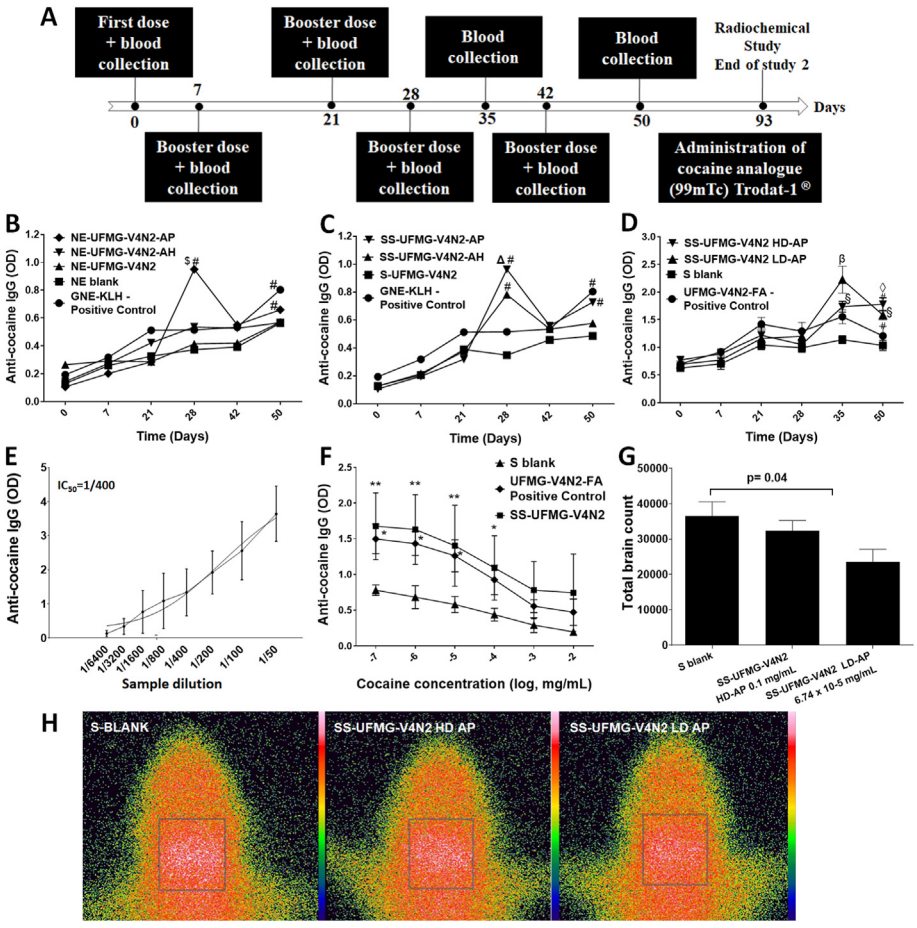

Fig. 3. *In vivo* studies. A Timeline of the two immunization protocols, the first and second protocols differed only by the collection on day 35 (optimization of the second study) and by the radiochemical study on day 93 (43 days after the last boost of the second protocol). **B, C** Study I. Anti-cocaine IgG antibodies levels in serum samples from BALB/C mice, immunized with UFMG-V4N2 delivered in **(B)** nanoemulsion (NE) and **(C)** solution (S)/suspensions (SS). Treatments: GNE-KLH (positive control), NE without UFMG-V4N2 (NE-blank), NE loaded with UFMG-V4N2 (NE-UFMG-V4N2), NE-V4N2 with aluminum hydroxide (NE-UFMG-V4N2-AH), NE-UFMG-V4N2 with aluminum phosphate (NE-UFMG-V4N2-AP), S loaded with UFMG-V4N2 (S-UFMG-V4N2), SS-UFMG-V4N2 with AH (SS-UFMG-V4N2-AH), SS-UFMG-V4N2 with AP (SS-UFMG-V4N2-AP). **D** Study II. Anti-cocaine IgG antibody levels in serum samples from BALB/C mice, immunized with UFMG-V4N2 at two different doses. Treatments: solution without UFMG-V4N2 (S blank), UFMG-V4N2 in Freund's adjuvant (UFMG-V4N2-FA, positive control), solution loaded with the lowest dose of UFMG-V4N2 (6.74×10^{-5} mg/mL) and AP (SS-UFMG-V4N2 LD-AP), solution loaded with the highest dose of UFMG-V4N2 (0.1 mg/mL) and AP (SS-UFMG-V4N2 HD-AP). **E** Study II. Determination of the midpoint anti-cocaine IgG antibodies titer in animals immunized with the SS-UFMG-V4N2-LD-AP. **F** Study II. Determination of the specificity of anti-cocaine antibodies in the serum of animals immunized with SS-UFMG-V4N2-LD-AP using adsorption ELISA technique. **G**, **H** Radiochemical study. Quantitative (**G**) and qualitative (**H**) results from radioactivity uptake of ^{99m}Tc-Trodat-1®, a radiolabeled cocaine analog, in the brain tissue of immunized and non-immunized BALB/c mice. OD: optical density. $^{\#}$Significant difference from day 0. $^{\$}$Significant difference from the NE-blank and NE-UFMG-V4N2. $^{\Delta}$Significant difference from the S-UFMG-V4N2 group. $^{\beta}$Significant difference from the other groups. §Significant difference from the placebo (S-blank). $^{\Diamond}$Significant difference from the placebo group and UFMG-V4N2-FA (positive control) group. *p ≤ 0.05, **p ≤ 0.005.

blood-brain barrier of these animals by means scintigraphy analysis. Fig. 3G and H shows, respectively, the quantitative and qualitative results of the analysis of scintigraphic images obtained from immunized mice and a lower radioactivity uptake was observed in the brain tissue of animals immunized with UFMG-V4N2 compared to the placebo group: SS-UFMG-V4N2 LD-AP < SS-UFMG-V4N2 HD-AP < S-blank. However, a statistical difference was observed only between the placebo and SS-V4N2 LD-AP groups ($p = 0.040$), evidencing a more effective uptake blockade for the lowest dose of UFMG-V4N2.

4. Discussion

Despite efforts to develop a vaccine for the treatment of disorders caused by cocaine [3,5,6], we still do not have a formulation registered with health surveillance agencies. Therefore, new strategies like the one we describe here are being evaluated. In this study, we 1. Characterized three batches of UFMG-V4N2 using different techniques; 2. Developed two pharmaceutical formulations (NEs and SSs) with excipients approved for parenteral use in humans, 3. Compared the immunogenicity of NEs and SSs and the use of AH and AP adjuvants; and 4. Also evaluated the most immunogenic dose of UFMG-V4N2 in the most promising formulation.

These are essential steps during the development of a new vaccine for human use. As UFMG-V4N2 is a new molecule, it needs to be characterized and the characteristics must be reproducible between batches. UFMG-V4N2 was synthesized because small molecules, such as cocaine, need a hapten (GNE) and a carrier (calixarene) to be effectively presented to the immune system. Thus, the immune system will be able to eliminate/neutralize it. Moreover, to administer UFMG-V4N2 in the human body, it is necessary to develop and characterize a pharmaceutical formulation composed of excipients and adjuvants approved for use in humans. For small molecules such as cocaine, the immune system uses antibodies to eliminate/neutralize it. If the body has anti-cocaine IgG antibodies, they will be able to bind cocaine, preventing it from passing through the blood-brain barrier [19,20]. For this reason, the developed formulations were injected into the animals and evaluated for their ability to induce the production of anti-cocaine IgG antibodies. Finally, for the most promising formulation, we not only quantified anti-cocaine IgG antibodies but also challenged their ability to reduce the passage of cocaine into the animals' brains. If fewer receptors are occupied in the brain with cocaine, there will be less pleasure and pharmacological effects [21,22]. Substantial blocking of cocaine's pleasurable effects helps reduce subsequent cravings, preventing the resumption. Thus, the initial blocking of the drug's effects in a single dose is the main objective of vaccines that seek to help addicts stay away from the abused substance, inhibiting the reinforcement of drug-seeking behavior, which can occur from social stresses that lead to exposure to cocaine, especially in the first few months after withdrawal [23,24].

UFMG-V4N2 showed characteristics of amorphous substances in polarized light microscopy, DSC and XRD analyses, probably due to the functionalization of calix [4]arene with four GNE hapten units, which was also observed for other functionalized calixarenes [25,26]. XRD results are in agreement with those obtained in DSC analyses, where broader endothermic curves were observed, characteristic of amorphous substances [27,28]. All analyzed batches showed similar patterns in the analyses, evidencing the synthesis reproducibility. The thermal stability observed in the TG and DSC analyses is consistent with that described in the literature for calix [4]arenes [29,30].

The SEM images of UFMG-V4N2 showed particles with irregular, heterogeneous structures and a wide range of particle sizes (approximately 523 to 2 μM), as described by other functionalized calix [4]arene [29]. Regarding solubility, UFMG-V4N2 showed a hydrophobic pattern, therefore, we used the association of surfactants, co-solvents and solvents to solubilize it in formulations. This is a common strategy to improve the solubility and bioavailability of hydrophobic drugs [31,32].

After pre-formulation studies, the formulations were developed and characterized (size, PDI, ZP, appearance, osmolality and pH). The addition of aluminum salts, mainly AP, caused an increase in the mean size of the NE globules, which remained below 300 nm (Fig. 3). This increase occurred because aluminum salts have a larger average particle size, around 1000 nm for AH and 2000 nm for AP [33]; and tend to aggregate to minimize surface free energy [34]. However, this increase was smaller than that observed by Eidi et al. [35], where modified fluorescent nanodiamonds complexed with AH had the mean particle size increased from 80 ± 30 nm to 2930 ± 230 nm.

The mean particle size of SS-UFMG-V4N2-AP (2470 ± 54 nm) and SS-UFMG-V4N2-AH (1407 ± 6 nm) reflects the mean particle size described for AP (2054 ± 54) and AH (1257 ± 54) [36]; since before the addition of aluminum salts we had a solution of UFMG-V4N2. In NE, the interaction between globules and aluminum salts minimized the aggregation process usually present [34,37]. Additionally, the higher concentration of surfactant in the NE (approximately 3x) may also have contributed to a lower aggregation and maintenance of the average size about 8 times smaller.

Regarding PDI, all formulations showed values close to 0.3, which suggests a monodisperse system [17]. The ZP is another critical parameter to be evaluated in parenteral formulations; and except for NE-UFMG-V4N2-AH, all formulations presented the ZP $\geq|20|$mV, which helps to stabilize the particles through electrical repulsion [38]. However, other factors can also minimize the aggregation process, such as steric stabilizers, like polysorbates [39], used in all formulations.

Like proteins, metallic hydroxyls exhibit an isoelectric point (IP). The IP of AH is around 9.4, with a positive charge at physiological pH; while the AP has the IP around 4.3, being negatively charged at physiological pH [33,40]. In SSs, only the particles of aluminum salts are in suspension, since the UFMG-V4N2 and excipients were utterly solubilized. Therefore, the SSs presented the ZP characteristic of aluminum salts, being positive for SS-UFMG-V4N2-AH (25 ± 4 mV) and negative for SS-UFMG-V4N2-AP (−20 ± 1 mV). In NEs, the negative charge was maintained, but for NE with AH, we observed a neutralization of the ZP. Orr et al. [41] also describe negative ZP (−18 ± 3 mV) for formulations with poly (acrylic acid) polymer and AH at pH around 7. Regarding the osmolarity, the NEs presented similar values to the plasma osmolarity (290 mOsm/kg), which can avoid pain and burning sensation at the time of administration [18]. However, all SSs had higher osmolarity values (2424 ± 58 mOsm/kg), which can be explained by the presence of 18% propylene glycol in formulations [42]. High osmolarity values are also observed in different parenteral drugs, such as phenobarbital, diazepam, and etomidate [42,43].

In the *in vivo* efficacy studies, only adjuvants (AP vs. AH) and the dose of UFMG-V4N2 (0.1 mg/mL vs. 6.74×10^{-5} mg/mL) significantly improved the anti-cocaine IgG antibody production. In the study 1 (Fig. 3A–C), no statistical differences were observed between NEs and SSs, but a trend toward higher anti-cocaine IgG antibody titers for AP formulations was observed. The better immunogenicity provided by formulations with AP may be related to the greater interaction between UFMG-V4N2 and AP particles. In solution, the UFMG-V4N2 nitrogens have a positive charge, favoring the adsorption of AP, which has a negative surface charge. The electrostatic adsorption process is well described in the literature as an important factor to increase the vaccines' immunogenicity [40,44].

Although some studies report a trend towards improved immunogenicity for nanoparticles compared to microparticles [10,45], no difference was observed for animals immunized with NEs (mean size about eight times smaller than SSs). This result can be explained by the size range observed for the NEs and SSs, respectively, around 300 nm and 1.5–2.5 μm. Particles smaller than 10 μm favor the antigen internalization by APCs, which are essential to induce an adaptive immune response, inducing higher titers of high-affinity IgG antibodies [46]. Small and medium particles (0.5, 1 and 2 μm) are generally internalized in more significant numbers than larger particles (3 and 4.5 μm); and 2 μm particles may represent a singular case due to the topography of the macrophage membrane [47]. Macrophage membrane ruffles are specially tuned with an average curvature of approximately 2 μm [48]. Thus, although SSs have micrometric particles instead of nanometric ones, they are in a size range that favors the internalization process.

Even though larger particles with a positive surface charge may increase uptake by APCs [49], SS-UFMG-V4N2-AH (ZP = 25 ± 4) induced antibody titers similar to NE-UFMG-V4N2- AH (ZP = −5 ± 1). The absence of greater immunogenicity for SS-UFMG-V4N2-AH can be explained by the presence of adjuvant AH instead of AP, as discussed above. Therefore, in the present study, the type of adjuvant had the greatest influence on the production of anti-cocaine antibodies.

In our studies, the statistical difference ($p < 0.05$) was observed for both formulations with AP, which produced higher anti-cocaine antibody titers on days 28 and 50. At the end of the study (day 50), the mean titers for the group immunized with GNE-KLH were also high, probably due to the presence of KLH and FA in the formulation [50,51]. However, no statistical difference was observed in the antibody titers in the animals of these three groups (NE-UFMG-V4N2-AP, SS-UFMG-V4N2-AP and GNE-KLH).

Since AP resulted in higher anti-cocaine IgG titers, and no difference was observed between SS and NE, the SS with AP was selected for the second study due to the lower production cost, which may make the technology more accessible to patients [32]. Therefore, the second study (Fig. 3D) compared two doses of UFMG-V4N2. Like Neto and Maia et al. [9], the lowest dose of UFMG-V4N2 induced higher titers of anti-cocaine antibodies. In relation to day 0, from day 35 onwards, this group presented statistical differences in IgG anti-cocaine antibody titers ($p < 0.05$); and although on day 50 the group immunized with the highest dose had the highest antibody titer, it was not significantly different from animals immunized with SS-UFMG-V4N2 LD-AP ($p = 0.5734$). High antibody titers were also observed in animals immunized with UFMG-V4N2-FA in the initial days ($p < 0.05$), which can be explained by the greater immunogenic potential of FA compared to AP.

The higher titers of anti-cocaine IgG antibodies observed at the lowest dose of UFMG-V4N2 may be related to lower responsiveness to high concentrations. Excessive doses of immunogen can hinder or decrease the immune response [52]. This effect, called hormesis, has been demonstrated in immunotherapies using rapamycin and cyclophosphamide [53,54]; as well as in studies with the vaccine ChAdOx1 nCoV-19 for COVID 19 [55].

Regarding the observed midpoint antibody titers for mice immunized with SS-UFMG-V4N2 LD-AP (Fig. 3E), although it was lower (1:400) than the midpoint described in the literature for another anti-cocaine vaccine in development (1:25,000) [3], as well as in relation to the other two studies previously published by our group [4,9], it is in accordance with another type of vaccine [56].

It is relevant to point out that there are only two anti-cocaine vaccines registered on ClinicalTrials.gov, the TA-CD vaccine and the dAd5GNE

vaccine. For the TA-CD vaccine, the phase II study was completed, but the results showed that the vaccine did not induce sufficient antibody titers in a population of drug addicts. Phase I results for the dAd5GNE vaccine have not yet been published, with completion scheduled for December 2025 [57,58]. Therefore, these results point to the need to develop new strategies, such as the one described here. Additionally, we must consider that the proposal presented in this work differs from the proposals described for these two immunotherapies, which are composed of components of biological origin. The dAd5GNE vaccine is comprised of a disrupted serotype 5 adenovirus gene therapy vector covalently conjugated to the cocaine analog GNE. TA-CD vaccine consists of succinylnorcocaine coupled to a recombinant cholera toxin B subunit. Although biological components present significant immunogenicity, they require cold chains for production and storage, as well as greater complexity in production and regulatory processing compared to synthetic substances [59,60].

In addition: 1. Unlike the present study, in the other studies the adjuvants used are not approved for human use, therefore, they do not constitute an adequate formulation to claim a clinical study; 2. As the anticocaine vaccines are still a new strategy, questions about the induction of high antibody titers have been raised. Should the vaccine help in the addiction control/elimination process or definitively restrict any action of cocaine in the body? 3. Despite the low antibody titers, a high specificity for cocaine was observed for antibodies from mice immunized with SS-UFMG-V4N2 LD-AP (Fig. 3F), which may explain the more effective blockade of radioactive cocaine analog [99 mTc]Trodat-1® uptake in the brain on scintigraphy analysis (Fig. 3G and H).

5. Conclusion

In this study, for the first time, an optimal formulation of an anticocaine vaccine was developed using only excipients and adjuvants approved for parenteral use in humans to carry UFMG-V4N2, an immunogen of chemical origin with good thermal stability. The developed formulation was characterized and shown to be capable of inducing the production of high-quality anti-cocaine IgG antibodies (high affinity for cocaine), reducing the entry of the radioactive cocaine analog [99 mTc] Trodat-1® into the brain. Therefore, the strengths of this vaccine formulation over other strategies are the use of a chemical immunogen, delivered in a formulation suitable for human administration and obtained by an easily scalable process, capable of generating a cocaine-specific IgG response, limiting cocaine delivery to the brain. Thus, our results open new perspectives for the development of chemical immunotherapy in the treatment of cocaine use disorder.

Funding

This study was partially supported by FAPEMIG (Fundação de Amparo à Pesquisa do Estado de Minas Gerais, Brazil) under grants APQ-02572-16 and APQ-04347-17; the National Council for Scientific and Technological Development, CNPq (Conselho Nacional de Desenvolvimento Tecnológico, Brazil) under grant 313944/2018–0; the Emenda Parlamentar Federal under grant 23970012; and Secretaria Nacional de Política sobre Drogas under grant 01/2017.

Declaration of competing interest

AF, FDG, GACG, and MCLN have stocks and are members of the advisory board of Hargon Ltd, a company dedicated to the development of new treatments for mental health.

Data availability

Data will be made available on request.

Acknowledgments

The authors would like to acknowledge the Center of Microscopy at UFMG (http://www.microscopia.ufmg.br) for providing the equipment and technical support for experiments involving SEM; to Hipolabor Farmacêutica LTDA (Rod BR 262 KM 12.3 - CEP 34.735–010. Borges/Sabará (MG), Brazil) for providing the equipment technical support for osmolality analyses; to Dr. Felipe Terra Martins and the Universidade Federal de Goias, UFG) for the support in the XRD experiments and Luiza de Lazari Ferreira (CTNano, Brazil) for the support in thermic analyzes.

References

[1] E. Colell, A. Domingo-Salvany, A. Espelt, O. Parés-Badell, M.T. Brugal, Differences in mortality in a cohort of cocaine use disorder patients with concurrent alcohol or opiates disorder, Addiction 113 (6) (2018) 1045–1055.
[2] M.H. Ozgen, S. Blume, The continuing search for an addiction vaccine, Vaccine 37 (36) (2019) 5485–5490.
[3] M.R.A. Carrera, J.A. Ashley, B. Zhou, P. Wirsching, G.F. Koob, K.D. Janda, Cocaine vaccines: antibody protection against relapse in a rat model, Proc. Natl. Acad. Sci. U. S. A. 97 (11) (2000) 6202–6206.
[4] P.S. de Almeida Augusto, R.L.G. Pereira, S.M. Caligiorne, B. Sabato, B.R.D. Assis, L.P. do Espírito Santo, K.D. Dos Reis, G.A.C. Goulart, Â. de Fátima, M.C.L. das Neves, F.D. Garcia, The GNE-KLH anti-cocaine vaccine protects dams and offspring from cocaine-induced effects during the prenatal and lactating periods, Mol. Psychiatr 26 (12) (2021) 7784–7791.
[5] M. Ramakrishnan, B.M. Kinsey, R.A. Singh, T.R. Kosten, F.M. Orson, Hapten optimization for cocaine vaccine with improved cocaine recognition, Chem. Biol. Drug Des. 84 (3) (2014) 354–363.
[6] S. Wee, M.J. Hicks, B.P. De, J.B. Rosenberg, A.Y. Moreno, S.M. Kaminsky, K.D. Janda, R.G. Crystal, G.F. Koob, Novel cocaine vaccine linked to a disrupted adenovirus gene transfer vector blocks cocaine psychostimulant and reinforcing effects, Neuropsychopharmacology 37 (5) (2012) 1083–1091.
[7] C. D'Amico, F. Fontana, R. Cheng, H.A. Santos, Development of vaccine formulations: past, present, and future, Drug Deliv Transl Res. 11 (2) (2021) 353–372.
[8] A.J. Pollard, E.M. Bijker, A guide to vaccinology: from basic principles to new developments, Nat. Rev. Immunol. 21 (2) (2021) 83–100.
[9] L. da Silva Neto, A.F. da Silva Maia, A.M. Godin, P.S. de Almeida Augusto, R.L.G. Pereira, S.M. Caligiorne, R.B. Alves, S.O.A. Fernandes, V.N. Cardoso, G.A.C. Goulart, F.T Martins, M.C.L. das Neves, F.D. Garcia, Â. de Fátima, Calix [n] arene-based immunogens: a new non-proteic strategy for anti-cocaine vaccine, J. Adv. Res. 38 (2021) 285–298.
[10] B.R.D. Assis, C.D. da Silva, M.G. Santiago, L.A.M. Ferreira, G.A.C. Goulart, Nanotechnology in adjuvants and vaccine development: what should we know? Nanomedicine 16 (29) (2021) 2565–2568.
[11] M. Jaiswal, R. Dudhe, P.K. Sharma, Nanoemulsion: an advanced mode of drug delivery system, 3 Biotech 5 (2) (2015) 123–127.
[12] H. HogenEsch, D.T. O'Hagan, C.B. Fox, Optimizing the utilization of aluminum adjuvants in vaccines: you might just get what you want, NPJ Vaccines 3 (2018) 51.
[13] X. Li, A.M. Aldayel, Z. Cui, Aluminum hydroxide nanoparticles show a stronger vaccine adjuvant activity than traditional aluminum hydroxide microparticles, J. Contr. Release 173 (2014) 148–157.
[14] F.a.D. Administration, CFR - code of federal regulations title 21. https://www.accessdata.fda.gov/scripts/cdrh/cfdocs/cfcfr/cfrsearch.cfm?fr=610.15, 2020. (Accessed 6 April 2021).
[15] U. Pharmacopeia, in: The United States Pharmacopeia and the National Formulary, 23rd and eighteenth ed., The United States Pharmacopeial Convention, Rockville, MD, 1994, p. 1456.
[16] R.C. Rowe, P. Sheskey, M. Quinn, Handbook of Pharmaceutical Excipients, Libros Digitales-Pharmaceutical Press, 2009.
[17] L. De Silva, J.Y. Fu, T.T. Htar, S. Muniyandy, A. Kasbollah, W.H.B. Wan Kamal, L.H. Chuah, Characterization, optimization, and in vitro evaluation of Technetium-99m-labeled niosomes, Int. J. Nanomed. 14 (2019) 1101–1117.
[18] P. Nony, P. Girard, S. Chabaud, L. Hessel, C. Thébault, J.P. Boissel, Impact of osmolality on burning sensations during and immediately after intramuscular injection of 0.5 ml of vaccine suspensions in healthy adults, Vaccine 19 (27) (2001) 3645–3651.
[19] A.J. Jenkins, R.M. Keenan, J.E. Henningfield, E.J. Cone, Correlation between pharmacological effects and plasma cocaine concentrations after smoked administration, J. Anal. Toxicol. 26 (7) (2002) 382–392.
[20] F.M. Orson, B.M. Kinsey, R.A. Singh, Y. Wu, T. Gardner, T.R. Kosten, The future of vaccines in the management of addictive disorders, Curr. Psychiatr. Rep. 9 (5) (2007) 381–387.
[21] R.L. Balster, C.R. Schuster, Fixed-interval schedule of cocaine reinforcement: effect of dose and infusion duration, J. Exp. Anal. Behav. 20 (1) (1973) 119–129.
[22] E.A. Minogianis, W.M. Shams, O.S. Mabrouk, J.T. Wong, W.G. Brake, R.T. Kennedy, P. du Souich, A.N. Samaha, Varying the rate of intravenous cocaine infusion influences the temporal dynamics of both drug and dopamine concentrations in the striatum, Eur. J. Neurosci. 50 (3) (2019) 2054–2064.

[23] R. Sinha, M. Garcia, P. Paliwal, M.J. Kreek, B.J. Rounsaville, Stress-induced cocaine craving and hypothalamic-pituitary-adrenal responses are predictive of cocaine relapse outcomes, Arch. Gen. Psychiatr. 63 (3) (2006) 324–331.
[24] A.K. Kexel, B. Kluwe-Schiavon, M.R. Baumgartner, E.J.E. Engeli, M. Visentini, C. Kirschbaum, E. Seifritz, B. Ditzen, L.M. Soravia, B.B. Quednow, Cue-induced cocaine craving enhances psychosocial stress and vice versa in chronic cocaine users, Transl. Psychiatry 12 (1) (2022) 443.
[25] L.U. Khan, H.F. Brito, J. Hölsä, K.R. Pirota, D. Muraca, M.C. Felinto, E.E. Teotonio, O.L. Malta, Red-green emitting and superparamagnetic nanomarkers containing Fe3O4 functionalized with calixarene and rare earth complexes, Inorg. Chem. 53 (24) (2014) 12902–12910.
[26] M. Tabakci, S. Erdemir, M. Yilmaz, Preparation, characterization of cellulose-grafted with calix[4]arene polymers for the adsorption of heavy metals and dichromate anions, J. Hazard Mater. 148 (1–2) (2007) 428–435.
[27] G. Shete, V. Puri, L. Kumar, A.K. Bansal, Solid state characterization of commercial crystalline and amorphous atorvastatin calcium samples, AAPS PharmSciTech 11 (2) (2010) 598–609.
[28] E.O. Kissi, K. Khorami, T. Rades, Determination of stable Co-amorphous drug-drug ratios from the eutectic behavior of crystalline physical mixtures, Pharmaceutics 11 (12) (2019) 628.
[29] I.A. Veesar, I.B. Solangi, S. Memon, Immobilization of α-amylase onto a calix [4] arene derivative: evaluation of its enzymatic activity, Bioorg. Chem. 60 (2015) 58–63.
[30] W. Yang, M.M. de Villiers, Aqueous solubilization of furosemide by supramolecular complexation with 4-sulphonic calix[n]arenes, J. Pharm. Pharmacol. 56 (6) (2004) 703–708.
[31] G. Krishna, W.F. Hodnick, W. Lang, X. Lin, S. Karra, J. Mao, B. Almassian, Pharmaceutical development and manufacturing of a parenteral formulation of a novel antitumor agent, VNP40101M, AAPS PharmSciTech 2 (3) (2001) E14.
[32] P. van Hoogevest, X. Liu, A. Fahr, Drug delivery strategies for poorly water-soluble drugs: the industrial perspective, Expet Opin. Drug Deliv. 8 (11) (2011) 1481–1500.
[33] M. Mold, E. Shardlow, C. Exley, Insight into the cellular fate and toxicity of aluminium adjuvants used in clinically approved human vaccinations, Sci. Rep. 6 (2016), 31578.
[34] I.Z. Romero Méndez, Y. Shi, H. HogenEsch, S.L. Hem, Potentiation of the immune response to non-adsorbed antigens by aluminum-containing adjuvants, Vaccine 25 (5) (2007) 825–833.
[35] H. Eidi, M.O. David, G. Crépeaux, L. Henry, V. Joshi, M.H. Berger, M. Sennour, J. Cadusseau, R.K. Gherardi, P.A. Curmi, Fluorescent nanodiamonds as a relevant tag for the assessment of alum adjuvant particle biodisposition, BMC Med. 13 (2015) 144.
[36] E. Shardlow, M. Mold, C. Exley, From stock bottle to vaccine: elucidating the particle size distributions of aluminum adjuvants using dynamic light scattering, Front. Chem. 4 (2016) 48.
[37] S. Shirodkar, R.L. Hutchinson, D.L. Perry, J.L. White, S.L. Hem, Aluminum compounds used as adjuvants in vaccines, Pharm. Res. (N. Y.) 7 (12) (1990) 1282–1288.
[38] N. Kathe, B. Henriksen, H. Chauhan, Physicochemical characterization techniques for solid lipid nanoparticles: principles and limitations, Drug Dev. Ind. Pharm. 40 (12) (2014) 1565–1575.
[39] S. Das, A. Chaudhury, Recent advances in lipid nanoparticle formulations with solid matrix for oral drug delivery, AAPS PharmSciTech 12 (1) (2011) 62–76.
[40] M. Huang, W. Wang, Factors affecting alum-protein interactions, Int. J. Pharm. 466 (1–2) (2014) 139–146.
[41] M.T. Orr, A.P. Khandhar, E. Seydoux, H. Liang, E. Gage, T. Mikasa, E.L. Beebe, N.D. Rintala, K.H. Persson, A. Ahniyaz, D. Carter, S.G. Reed, C.B. Fox, Reprogramming the adjuvant properties of aluminum oxyhydroxide with nanoparticle technology, NPJ Vaccines 4 (2019) 1.
[42] A. Doenicke, A.E. Nebauer, R. Hoernecke, M. Mayer, M.F. Roizen, Osmolalities of propylene glycol-containing drug formulations for parenteral use. Should propylene glycol be used as a solvent? Anesth. Analg. 75 (3) (1992) 431–435.
[43] H. Bretschneider, Osmolalities of commercially supplied drugs often used in anesthesia, Anesth. Analg. 66 (4) (1987) 361–362.
[44] C. Vessely, T. Estey, T.W. Randolph, I. Henderson, R. Nayar, J.F. Carpenter, Effects of solution conditions and surface chemistry on the adsorption of three recombinant botulinum neurotoxin antigens to aluminum salt adjuvants, J. Pharmacol. Sci. 96 (9) (2007) 2375–2389.
[45] R.R. Shah, D.T. O'Hagan, M.M. Amiji, L.A. Brito, The impact of size on particulate vaccine adjuvants, Nanomedicine 9 (17) (2014) 2671–2681.
[46] G.L. Morefield, A. Sokolovska, D. Jiang, H. HogenEsch, J.P. Robinson, S.L. Hem, Role of aluminum-containing adjuvants in antigen internalization by dendritic cells in vitro, Vaccine 23 (13) (2005) 1588–1595.
[47] P. Pacheco, D. White, T. Sulchek, Effects of microparticle size and Fc density on macrophage phagocytosis, PLoS One 8 (4) (2013), e60989.
[48] J.A. Champion, A. Walker, S. Mitragotri, Role of particle size in phagocytosis of polymeric microspheres, Pharm. Res. (N. Y.) 25 (8) (2008) 1815–1821.
[49] C. Foged, B. Brodin, S. Frokjaer, A. Sundblad, Particle size and surface charge affect particle uptake by human dendritic cells in an in vitro model, Int. J. Pharm. 298 (2) (2005) 315–322.
[50] S. Apostólico Jde, V.A. Lunardelli, F.C. Coirada, S.B. Boscardin, D.S. Rosa, Adjuvants: classification, modus operandi, and licensing, J Immunol Res 2016 (2016), 1459394.
[51] A. Swaminathan, R.M. Lucas, K. Dear, A.J. McMichael, Keyhole limpet haemocyanin - a model antigen for human immunotoxicological studies, Br. J. Clin. Pharmacol. 78 (5) (2014) 1135–1142.
[52] J.E. Eyles, E.D. Williamson, H.O. Alpar, Immunological responses to nasal delivery of free and encapsulated tetanus toxoid: studies on the effect of vehicle volume, Int. J. Pharm. 189 (1) (1999) 75–79.
[53] K. Araki, A.H. Ellebedy, R. Ahmed, TOR in the immune system, Curr. Opin. Cell Biol. 23 (6) (2011) 707–715.
[54] A. Gaya, C.A. Akle, S. Mudan, J. Grange, The concept of hormesis in cancer therapy - is less more? Cureus 7 (4) (2015) e261.
[55] M. Voysey, S.A.C. Clemens, S.A. Madhi, L.Y. Weckx, P.M. Folegatti, P.K. Aley, B. Angus, V.L. Baillie, S.L. Barnabas, Q.E. Bhorat, S. Bibi, C. Briner, P. Cicconi, A.M. Collins, R. Colin-Jones, C.L. Cutland, T.C. Darton, K. Dheda, C.J.A. Duncan, K.R.W. Emary, K.J. Ewer, L. Fairlie, S.N. Faust, S. Feng, D.M. Ferreira, A. Finn, A.L. Goodman, C.M. Green, C.A. Green, P.T. Heath, C. Hill, H. Hill, I. Hirsch, S.H.C. Hodgson, A. Izu, S. Jackson, D. Jenkin, C.C.D. Joe, S. Kerridge, A. Koen, G. Kwatra, R. Lazarus, A.M. Lawrie, A. Lelliott, V. Libri, P.J. Lillie, R. Mallory, A.V.A. Mendes, E.P. Milan, A.M. Minassian, A. McGregor, H. Morrison, Y.F. Mujadidi, A. Nana, P.J. O'Reilly, S.D. Padayachee, A. Pittella, E. Plested, K.M. Pollock, M.N. Ramasamy, S. Rhead, A.V. Schwarzbold, N. Singh, A. Smith, R. Song, M.D. Snape, E. Sprinz, R.K. Sutherland, R. Tarrant, E.C. Thomson, M.E. Török, M. Toshner, D.P.J. Turner, J. Vekemans, T.L. Villafana, M.E.E. Watson, C.J. Williams, A.D. Douglas, A.V.S. Hill, T. Lambe, S.C. Gilbert, A.J. Pollard, Safety and efficacy of the ChAdOx1 nCoV-19 vaccine (AZD1222) against SARS-CoV-2: an interim analysis of four randomised controlled trials in Brazil, South Africa, and the UK, Lancet 397 (10269) (2021) 99–111.
[56] A.H. Chou, C.C. Liu, J.Y. Chang, S.P. Lien, M.S. Guo, H.P. Tasi, K.N. Hsiao, S.J. Liu, C. Sia, S.C. Wu, M.S. Lee, C.H. Hsiao, J.R. Wang, Y.H. Chow, P. Chong, Immunological evaluation and comparison of different EV71 vaccine candidates, Clin. Dev. Immunol. 2012 (2012), 831282.
[57] B.A. Martell, F.M. Orson, J. Poling, E. Mitchell, R.D. Rossen, T. Gardner, T.R. Kosten, Cocaine vaccine for the treatment of cocaine dependence in methadone-maintained patients A randomized, double-blind, placebo-controlled efficacy trial, Arch. Gen. Psychiatr. 66 (10) (2009) 1116–1123.
[58] W.M.C.o.C. University, Safety study of a disrupted adenovirus (Ad) serotype cocaine vaccine for cocaine-dependent individuals. https://clinicaltrials.gov/ct2/show/NCT02455479, 2022. (Accessed 10 November 2022).
[59] M.M. Naseer, M. Ahmed, S. Hameed, Functionalized calix [4] arenes as potential therapeutic agents, Chem. Biol. Drug Des. 89 (2) (2017) 243–256.
[60] R. Zhang, B.D. Ulery, Synthetic vaccine characterization and design, J. Bionanoscience 12 (1) (2018) 1–11.